

Use Short Isometric Shapelets to Accelerate Binary Time Series Classification

Weibo Shu · Yaqiang Yao ·
Shengfei Lyu · Jinlong Li ·
Huanhuan Chen

Received: date / Accepted: date

Abstract In the research area of time series classification, the ensemble shapelet transform algorithm is one of state-of-the-art algorithms for classification. However, its high time complexity is an issue to hinder its application since its base classifier shapelet transform includes a high time complexity of a distance calculation and shapelet selection. Therefore, in this paper we introduce a novel algorithm, i.e. short isometric shapelet transform, which contains two strategies to reduce the time complexity. The first strategy of SIST fixes the length of shapelet based on a simplified distance calculation, which largely reduces the number of shapelet candidates as well as speeds up the distance calculation in the ensemble shapelet transform algorithm. The second strategy is to train a single linear classifier in the feature space instead of an ensemble classifier. The theoretical evidences of these two strategies are presented to guarantee a near-lossless accuracy under some preconditions while reducing the time complexity. Furthermore, empirical experiments demonstrate the superior performance of the proposed algorithm.

Keywords Time Series Classification · Feature Selection · Feature Space · Machine Learning

Weibo Shu
E-mail: weiboshu@mail.ustc.edu.cn

Yaqiang Yao
E-mail: yaoyaq@mail.ustc.edu.cn

Shengfei Lyu
E-mail: saintfe@mail.ustc.edu.cn

Jinlong Li
E-mail: jlli@ustc.edu.cn

Huanhuan Chen
E-mail: hchen@ustc.edu.cn
University of Science and Technology of China, Hefei, Anhui, China

1 Introduction

Time series are one type of multidimensional data with a wide range of applications in economy, medical treatments, and engineering [14; 20]. The ordered values in time series contain abundant latent information of data, which makes time series analysis a challenging task. Time series classification (TSC) plays a significant role in time series analysis [13; 47]. It appears in a number of new scenarios such as text retrieval [1], fault diagnosis [38; 15], and bioinformatics [19].

Many algorithms were proposed to tackle TSC problems during the last decades. The existing algorithms of TSC can be roughly categorized into the following five categories [3]. The first category is based on the similarity between two time series. Several bespoke distance metrics between pairwise time series were designed to measure the similarity between two time series. Further, the classification relies on these specific distance metrics [37; 39; 27; 36; 46; 22; 5; 21; 33]. In contrast to the algorithms based on whole series, the second category focuses on extracting local features of time series to classify them [40; 18; 7; 6; 48; 29; 23]. The third category transforms time series into strings by a uniform dictionary and then measures by the similarity among these strings [31; 42; 32; 43; 41]. The fourth category is model-based algorithms that represent time series with models and then conduct classification on these models [45; 17; 16; 30; 20; 4]. The last category tries to transform source data into a new feature space and then classify them in the new feature space [28; 25; 8; 2; 34; 44]. Based on the aforementioned algorithms as base classifiers, ensemble algorithms [33; 18; 41; 34] can be built to generate a committee for possible better performance [10; 11; 12], since they try to employ accurate yet diverse multiple.

These various algorithms are often related with each other. In the second category of algorithms, shapelets proposed in [48] are subseries with informative features, and they can be used to build a decision tree where the attribute of each node is the distance between time series and a selected shapelet. Based on informative shapelets, shapelet transform (ST) constructs a feature space and carries out a classification in this feature space [25]. Finally, the ensemble shapelet transform algorithm achieves the state-of-the-art in terms of classification accuracy by including a number of base classifiers – shapelet transform [3; 25; 8].

However, the high computational complexity of the shapelet transform is severe to hinder the application of its ensemble algorithms. On one hand, in the base classifier, a basic manipulation is calculating the distance between a shapelet and a time series. The distance between a shapelet denoted by \mathbf{s} and a time series denoted by \mathbf{x} is calculated by the following formula [48]:

$$Dist(\mathbf{s}, \mathbf{x}) = \min \left\{ d(\mathbf{s}, P) \mid P = (x_i, \dots, x_{i+k-1}), \right. \\ \left. i = 1, \dots, m - k + 1 \right\} \quad (1)$$

where $d(\cdot, \cdot)$ is the function of Euclidean Distance, P is a continuous subsequence, m is the length of time series \mathbf{x} , and k is the length of shapelet \mathbf{s} .

This formula also serves as the distance calculation formula between shapelet candidates and time series. And the time complexity of a distance calculation is $\mathcal{O}(k(m-k))$, a quadratic item of the length of shapelet. On the other hand, shapelets are selected from shapelets candidates which are all the subseries of all the time series. For a n -size and m -length time series set, there are $\frac{nm(1+m)}{2}$ candidates in the shapelet transform algorithm.

To tackle this issue, the short isometric shapelet transform (SIST) algorithm is proposed to reduce the time complexity of the ensemble shapelet transform algorithm in this paper. First, SIST fixes the length of shapelet based on a simplified distance calculation, which largely reduces the number of shapelet candidates as well as speeds up the distance calculation in the ensemble shapelet transform algorithm. In addition, SIST substitutes the ensemble classifier with a single classifier in the shapelet-based feature space, which will sharply decrease training time of the classifier. The theoretical evidences are given to demonstrate that the two strategies can guarantee the reduction of time complexity with the near-lossless accuracy. Furthermore, SIST empirically achieves a promising accuracy on most of binary data sets, which shows its effectiveness.

The rest of the paper is organized as follows. The background and outline of SIST are introduced in Section 2. Theoretical analysis about the proposed strategies in SIST is presented in Section 3. Section 4 shows empirical results of the proposed algorithm and Section 5 concludes this paper.

2 Short Isometric Shapelet Transform

2.1 Time Shapelet

Firstly, two basic terminologies are given as follows:

time series data

One sample of time series consists of an ordered multi-dimensional value and a corresponding class label. It is normally expressed with (\mathbf{x}, y) , where \mathbf{x} is an vector and y is the class label. The whole time series are denoted by $(\mathbf{X}, \mathbf{Y}) = ((\mathbf{x}_1, y_1), (\mathbf{x}_2, y_2), \dots, (\mathbf{x}_n, y_n))$. In general, time series in a data set are isometric after the preliminary processing.

shapelet

The shapelet is the discriminative subseries derived from time series [48]. Subseries are continuous subsequences in time series. A shapelet is expressed with (\mathbf{s}, z) , where \mathbf{s} is the subseries and z is the class label from its original time series. In a shapelet-based algorithm, each shapelet usually represents a local feature.

Shapelets are selected from the candidates that comprise every subseries of all the time series. There are four steps to choose informative shapelets. In the first step, for each shapelet candidate, distances from it to all the time series are calculated. After that, a prime segmentation is explored on the real

number axis where all the calculated distances are marked. Then by classifying time series according to the divided segments which their corresponding distances fall in, time series are divided into some disjoint subsets. Subsequently, the information gain is calculated according to the division. Finally, shapelet candidates with better information gain are selected as shapelets.

In the first step, pairwise distances are calculated among the candidates. Then, a prime segmentation is explored on the real number axis where all the calculated distances are marked in the second step. Some disjoint subsets of the candidates are obtained by segmenting them in the third step. Finally, the information gain is calculated according to these disjoint subsets and those with better information gain are selected as shapelets.

Due to the substantial time spent in selecting shapelets by brute force, Ye and Keogh [48] exploited some tricks, for example early abandon, to reduce the time consumption. Several methods also tried to solve this time consumption problem [29; 23; 26]. Although to a certain extent time complexity has been reduced, there is some loss of accuracy.

2.2 Shapelet Transform (ST)

It uses a disposable selection to select k shapelets from all the shapelet candidates. Then it transforms original time series into a k -dimensional vector where the value of the i th dimension is the distance between the i th selected shapelet and time series.

This method exploits shapelets in a different way from constructing a decision tree. These shapelets are selected only once in this method, whereas the frequency of the shapelets selection equals the number of branch nodes of the decision tree in the algorithm of Ye and Keogh [48]. Hence, after this work, the key point of cutting time consumption are turning to selecting the top k most discriminative shapelet candidates as fast as possible [24; 9]. However, the time complexity is still high as a result of the large number of shapelet candidates as well as the complex distance calculation.

2.3 Short Isometric Shapelet Transform (SIST)

For clearly elucidating improvements by a comparison, SIST will be introduced with the ensemble ST algorithm (Fig. 1).

For a TSC problem, the first step of the ensemble ST algorithm is to extract all the subseries of each time series as shapelet candidates. But in SIST, only the subseries with a small fixed length will be extracted from each time series. Therefore, the number of shapelet candidates in SIST becomes fairly small compared with it in the ensemble ST algorithm. The validity of this strategy will be elaborated later. Step 1 of Fig. 1 illustrates the difference.

The second step is to select shapelets from shapelet candidates. According to the elaboration in Subsection 2.1, a process of exploring the prime

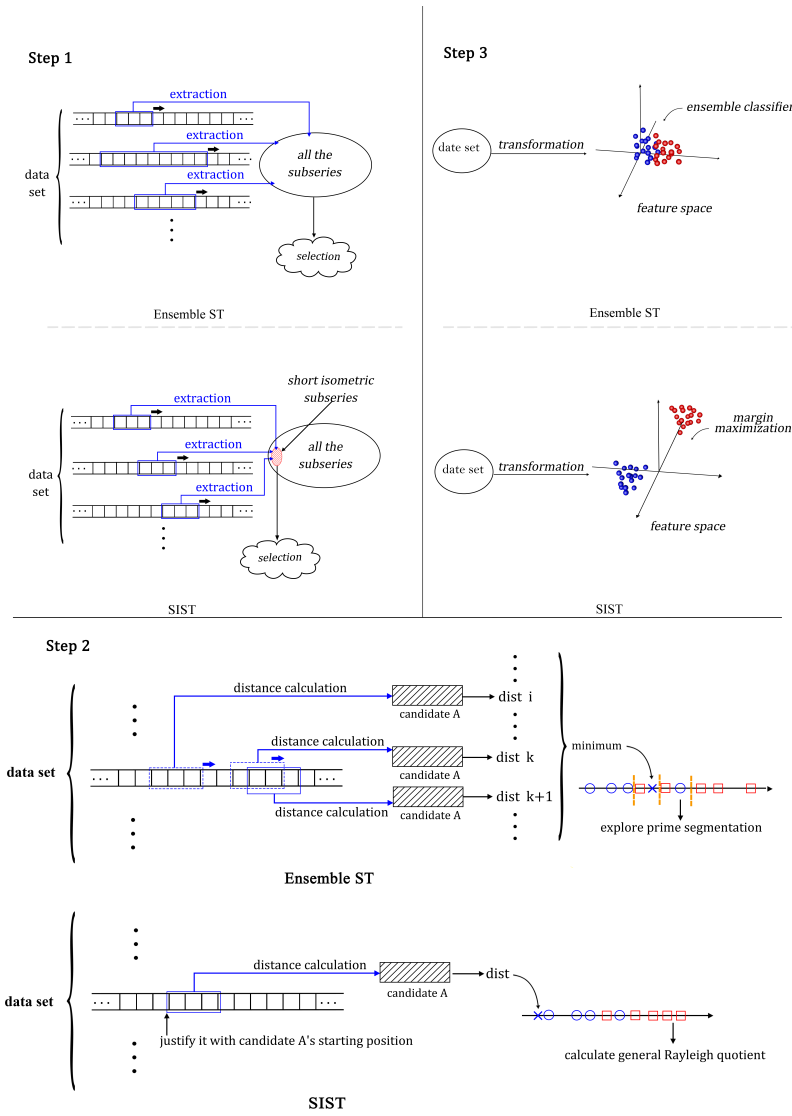


Fig. 1: Differences between the ensemble ST and SIST. Details of this figure are discussed in Subsection 2.3

segmentation in the real axis is indispensable in this step. But in SIST, this time-consuming process is removed by using the generalized Rayleigh quotient rather than the prime information gain as the discrimination index of shapelet candidates. Besides, the position of shapelet candidates in its original time series is exploited to simplify the distance calculation. Moreover, these

improvements will be justified later. And all these differences are illustrated in step 2 of Fig. 1.

In the ensemble ST algorithm, the final step is to transform source time series into vectors by selected shapelets (the transformation is described in 2.2) and then train an ensemble classifier in that vector space. But we claim that if shapelets are selected by using the generalized Rayleigh quotient of shapelet candidates as the selection priority, there is a high degree of the linear separability of the transformed data in the vector space. Consequently, only a single SVM is trained to classify data in SIST. Theoretical evidences to support this claim will be given later. Step 3 of Fig. 1 shows the difference in the final step. Furthermore, since shapelets are short and distance calculation is simplified in SIST, much time is saved in transforming time series into the feature space.

3 Theoretical Analysis

In this section, the theoretical evidence of the two proposed strategies in SIST will be elaborated. It can guarantee as small loss of accuracy as possible and reduce significantly time complexity. The content of this section is organized as follows. Firstly, the shapelet candidate extraction based on the proposed ‘Fixed Distance’ will be analyzed in Subsection 3.1 and 3.2. This part explains the feasibility of the first strategy that uses only the shapelet candidates with a small fixed length. This strategy will save time by largely reducing the number of shapelet candidates. Subsequently, the theoretical supports of the second strategy that substitutes the ensemble classifier with a single linear classifier, will be discussed in Subsection 3.3. This strategy will sharply cut the time consumption of the classifier training in the feature space. Finally, the algorithmic flow with the time complexity analysis is given in Subsection 3.4.

3.1 Simplification of the Distance Calculation

In typical shapelet-based algorithms, it is time-consuming to measure the distance between shapelets and time series. The high time complexity of one distance calculation is drastically amplified by the frequency of the distance calculation.

Hence a basic idea in this paper is to use the position information of shapelets to simplify the distance calculation shown in Eq. (1). Each shapelet or shapelet candidate is a subseries derived from an original time series in the data set. Therefore, its start point is a specific position in its original time series. The starting position can be used to simplify the distance calculation as the following ‘Fixed Distance’ shows.

$$Fixed_Dist(\mathbf{s}, \mathbf{x}) = \left\{ d(\mathbf{s}, P) \mid P = (x_i, \dots, x_{i+k-1}), \right. \quad (2)$$

$$\left. i = j \right\}$$

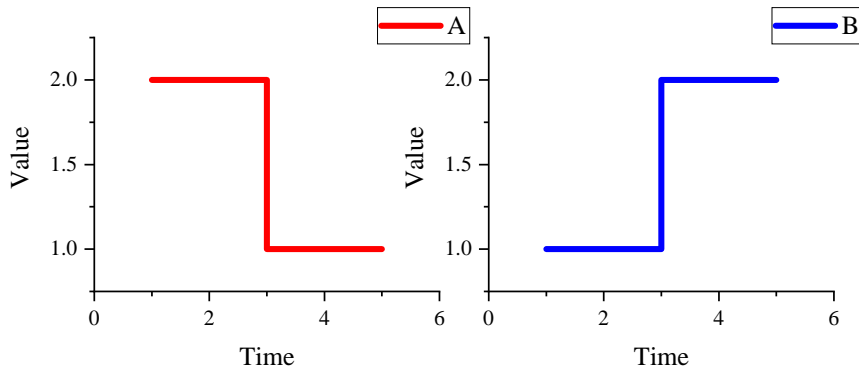


Fig. 2: Example of the usage of position information. The first half of class A can distinguish A and B by Eq. (2), whereas it can not do that by Eq. (1).

where j is the starting position of shapelet \mathbf{s} and other parameters are same with them in Eq. (1). It also serves as the distance calculation formula of shapelet candidates and time series. Based on Eqs. (1-2), the time complexity of a distance calculation has been changed from $\mathcal{O}(k(m-k))$ to $\mathcal{O}(k)$.

Both the information the local feature brings and the position where the local feature appears are focused on Fixed Distance in Eq. (2). Instead, only the former is concentrated on the typical distance metric in Eq. (1). Moreover, if distances between shapelets and time series are calculated by Eq. (2), much time is saved. One part of the saved time is evident from the comparison between Eq. (1) and Eq. (2). The other part is indirect, and details will be elaborated in Subsection 3.2. In that subsection, Fixed Distance plays an important role.

There is a simple example illustrating that Eq. (2) reinforces the discrimination ability of shapelets. Data A and B are shown in Fig. 2. If the first half of Data A is selected as a shapelet S , then by Eq. (1), the distance between S and A is 0 and the distance between S and B is also 0. However, if distances are calculated by Eq. (2), then the distance between S and A is 0 and the distance between S and B is $\sqrt{2}$. Hence, S can classify A and B by Eq. (2) whereas it can not do that by Eq. (1). That is because in Eq. (2), the distance calculation takes into account the position of the local feature represented by the shapelet. In Eq. (2), the distance calculation is fixed at the specific position marked by the start point of the shapelet. That's why it is called 'Fixed Distance'.

3.2 Short Isometric Shapelet Candidates

In this subsection, theoretical analysis focuses on fixing the length of shapelet candidates, namely the strategy showed in Step 1 of Fig. 1.

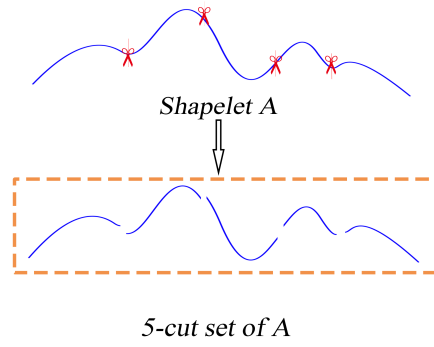


Fig. 3: Example of n -cut set.

In the process of selecting appropriate shapelets, the time of evaluating a single shapelet candidate is multiplied by the number of all the shapelet candidates. And the number of shapelet candidates is so substantial that the time consumption is huge. If it can be known about the prime length or even a small range of the prime length of shapelets, then shapelet candidates whose length are not the prime one can be discarded. And the huge time consumption vanishes as a result of the drastic reduction of the number of shapelet candidates. Generally speaking, it is hard to know the prime length, or the time spent in searching the best length is not less than the time it saves. However, in SIST, under the precondition that Fixed Distance is used as the distance calculation formula, the length of shapelet candidates can actually be fixed as a small number without an appreciation of the prime length. To explain this conclusion, firstly some conceptions should be strictly defined as follows:

Definition 1 Given a n -size set A of time series and a k -size set B of shapelets, the process of transforming each time series in A into a k -dimensional vector by metric d , which means the value at the i th dimension of the k -dimensional vector is the d metric from the time series to the i th shapelet in B , is called A 's **shapelet transform through B by metric d** .

Definition 2 Given a shapelet (s, z) , cut it in arbitrary $n - 1$ cut points to produce n ($n > 1$) subseries of (s, z) . Each subseries is a new shapelet derived from (s, z) and all of them constitute (s, z) . The set of the n new shapelets is called the **n -cut set** of (s, z) .

A simple example of n -cut set is shown in Fig. 3. Based on the aforementioned conceptions, a key proposition is given as follows:

Proposition 1 A is a vector set coming from a time series set B 's shapelet transform through a single shapelet (\mathbf{s}, z) by Fixed Distance, and C is another vector set coming from B 's shapelet transform through D by Fixed Distance too, here D is an arbitrary n -cut set of (\mathbf{s}, z) with any $n > 1$. Then for any time series in B , its corresponding vector in A has the same Euclidean norm with its corresponding vector in C .

Proof For any time series (\mathbf{x}, y) in set B , it's needed to prove that its shapelet transform through (\mathbf{s}, z) by Fixed Distance has the same Euclidean norm with its shapelet transform through any n -cut set D of (\mathbf{s}, z) by Fixed Distance.

The following is the representation of the time series \mathbf{x} , the shapelet \mathbf{s} , and the n -cut set D .

$$\mathbf{x} = (x_1, x_2, \dots, x_m) \quad (3a)$$

$$\mathbf{s} = (s_i, s_{i+1}, \dots, s_{i+k}) \quad 1 \leq i \leq m, \quad i+k \leq m \quad (3b)$$

$$D = \{\mathbf{s}_1, \mathbf{s}_2, \dots, \mathbf{s}_n\} \quad 1 \leq n \leq k+1 \quad (3c)$$

$$\begin{aligned} t_j &= \text{the terminal position of } \mathbf{s}_j \\ 1 \leq j \leq n, \quad i \leq t_1 < t_2 < \dots < t_n = i+k \end{aligned} \quad (3d)$$

$$\mathbf{s}_1 = (s_i, s_{i+1}, \dots, s_{t_1}) \quad (3e)$$

$$\mathbf{s}_h = (s_{t_{h-1}+1}, s_{t_{h-1}+2}, \dots, s_{t_h}) \quad 2 \leq h \leq n \quad (3f)$$

Next formulas represent the vectors transformed through \mathbf{s} and D respectively by Fixed Distance.

$$V_{\mathbf{x}/\mathbf{s}} = \left(\sqrt{\sum_{p=i}^{i+k} (x_p - s_p)^2} \right) \quad (4)$$

$$\begin{aligned} V_{\mathbf{x}/D} = & \left(\sqrt{\sum_{p=i}^{t_1} (x_p - s_p)^2}, \sqrt{\sum_{p=t_1+1}^{t_2} (x_p - s_p)^2}, \dots, \right. \\ & \left. \sqrt{\sum_{p=t_{n-1}+1}^{t_n} (x_p - s_p)^2} \right) \end{aligned} \quad (5)$$

The next step is to prove that these two vectors have the same Euclidean norm. Notice that if all the shapelets in D are concatenated in sequence then

the shapelet \mathbf{s} is acquired, hence,

$$\begin{aligned}
\|V_{\mathbf{x}/D}\|_2 &= \sqrt{\sum_{p=i}^{t_1} (x_p - s_p)^2 + \sum_{q=2}^n \sum_{p=t_{q-1}+1}^{t_q} (x_p - s_p)^2} \\
&= \sqrt{\sum_{p=i}^{t_n} (x_p - s_p)^2} \\
&= \sqrt{\sum_{p=i}^{i+k} (x_p - s_p)^2} \\
&= \|V_{\mathbf{x}/\mathbf{s}}\|_2
\end{aligned} \tag{6}$$

And this is exactly what is needed.

According to the shapelet transform defined in Definition 1, the word ‘norm’ in the Proposition 1 actually means the similarity measurement between the time series and the shapelets representing a local feature set of the class ‘ z ’. Therefore, in Proposition 1, for a very discriminative shapelet (\mathbf{s}, z) , the Euclidean norm of a corresponding vector of the time series whose class label is ‘ z ’ should be as small as possible, and it of the other vectors should be as large as possible (Here, the small value of similarity measurement means a high similarity and the big one means a low similarity). Hence, this proposition actually ensures that the similarity measurement is an invariant under those two different shapelet transform processes. An intuitive and simple example is shown in Fig. 4.

Furthermore, the following corollary can be proven based on Proposition 1.

Corollary 1 A is a vector set coming from a time series set B ’s shapelet transform through a shapelet set C by Fixed Distance, $D \subset C$, $E = \bigcup_{\mathbf{s} \in D} (n_{\mathbf{s}}\text{-cut set of } \mathbf{s})$, and $F = C - D \cup E$. G is another vector set coming from B ’s shapelet transform through F by Fixed Distance. Then for any time series in B , its corresponding vector in A has the same Euclidean norm with its corresponding vector in F .

Proof The proof begins with the following notation. C is a shapelet set represented as follows:

$$C = \{\mathbf{s}_1, \mathbf{s}_2, \dots, \mathbf{s}_m\}. \tag{7}$$

D is a subset of C , it is represented as follows:

$$D = \{\mathbf{s}_{k_1}, \mathbf{s}_{k_2}, \dots, \mathbf{s}_{k_l}\}. \tag{8}$$

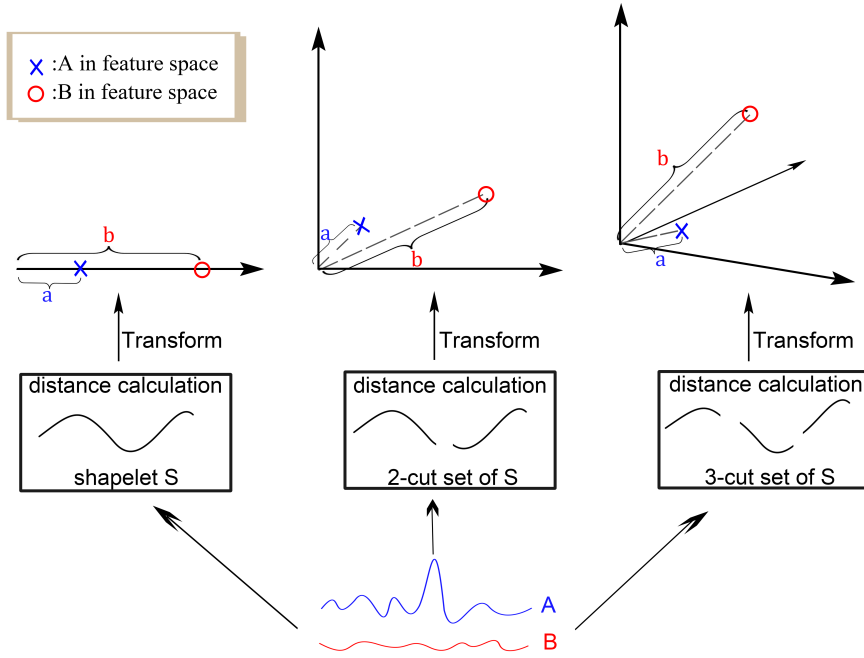


Fig. 4: An intuitive example to interpret Proposition 1. A and B are two time series, and they are transformed through a shapelet, its 2-cut set, and its 3-cut set respectively by Fixed Distance. Though A has different representative vectors in different feature spaces, these vectors keep the same length (the Euclidean norm) in different feature spaces. And so does B. Hence one keeps close to origin and the other keeps far from origin in all the three feature spaces.

E , as defined in the corollary, is the union set of all the n_s -cut sets of shapelets in D , and it is represented as follows:

$$E = \{\mathbf{s}_{k_1}^1, \dots, \mathbf{s}_{k_1}^{n_{k_1}}, \mathbf{s}_{k_2}^1, \dots, \mathbf{s}_{k_2}^{n_{k_2}}, \dots, \mathbf{s}_{k_l}^1, \dots, \mathbf{s}_{k_l}^{n_{k_l}}\}. \quad (9)$$

Besides, $C - D$ is represented as follows:

$$C - D = \{\mathbf{s}_{t_1}, \mathbf{s}_{t_2}, \dots, \mathbf{s}_{t_{m-l}}\}. \quad (10)$$

Hence, a time series \mathbf{x} 's shapelet transform through C and $C - D \cup E$ respectively by Fixed Distance are as follows:

$$V_{\mathbf{x}/C} = \begin{pmatrix} \|V_{\mathbf{x}/\mathbf{s}_{k_1}}\|_2, \dots, \|V_{\mathbf{x}/\mathbf{s}_{k_l}}\|_2, \\ \|V_{\mathbf{x}/\mathbf{s}_{t_1}}\|_2, \dots, \|V_{\mathbf{x}/\mathbf{s}_{t_{m-l}}}\|_2 \end{pmatrix}, \quad (11)$$

$$V_{\mathbf{x}/C-D\cup E} = \begin{pmatrix} \|V_{\mathbf{x}/s_{k_1}^1}\|_2, \dots, \|V_{\mathbf{x}/s_{k_1}^{n_{k_1}}}\|_2, \\ \dots \\ \|V_{\mathbf{x}/s_{k_l}^1}\|_2, \dots, \|V_{\mathbf{x}/s_{k_l}^{n_{k_l}}}\|_2, \\ \|V_{\mathbf{x}/s_{t_1}}\|_2, \dots, \|V_{\mathbf{x}/s_{t_{m-l}}}\|_2 \end{pmatrix}. \quad (12)$$

Now calculate Euclidean norm of these two vectors,

$$\begin{aligned} \|V_{\mathbf{x}/C}\|_2 &= \sqrt{\sum_{p=1}^l \|V_{\mathbf{x}/s_{k_p}}\|_2^2 + \sum_{q=1}^{m-l} \|V_{\mathbf{x}/s_{t_q}}\|_2^2} \\ &= \sqrt{\sum_{p=1}^l \sum_{r=1}^{n_{k_p}} \|V_{\mathbf{x}/s_{k_p}^r}\|_2^2 + \sum_{q=1}^{m-l} \|V_{\mathbf{x}/s_{t_q}}\|_2^2} \\ &= \|V_{\mathbf{x}/C-D\cup E}\|_2 \end{aligned} \quad (13)$$

The second equal sign is hold by Proposition 1. And this finishes the proof of Corollary 1.

According to this corollary and the analysis tightly after Proposition 1, if the approximate n -cut set of a shapelet (\mathbf{s}, z) is added as part of the shapelet basis used for the shapelet transform, then (\mathbf{s}, z) in itself can be dropped in that shapelet basis. That's because the classification in the feature space mainly relies on the similarity measurement between transformed data and selected local features. However, the shapelet transform reflects the similarity measurement on the norm of transformed vectors, and Corollary 1 guarantees the identical norms of transformed vectors in different feature spaces constructed by the two different shapelet basis. Hence, Corollary 1 actually says that the original shapelet basis and the changed shapelet basis can construct the nearly same feature space in terms of classification. Therefore, in a shapelet basis, the substitution of a shapelet with its n -cut set is feasible while the eventual purpose is classifying transformed data.

Every long shapelet consists of some short shapelets so that it must have an n -cut set including only short sub-shapelets. As stated above, Corollary 1 guarantees that all the shapelets can be replaced by their cut sets of short sub-shapelets. Therefore, selecting the elementary short shapelets is quite enough. Hence, the length of shapelet candidates can be fixed at a small number and these shapelet candidates are called 'short isometric shapelet candidates'.

After restricting the length of shapelet candidates to a small constant h , the number of shapelet candidates is cut to $n(m-h+1)$ for a n -size and m -length time series set while there are $\frac{nm(1+m)}{2}$ shapelet candidates in typical shapelet-dependent algorithms.

3.3 Substituting the Ensemble Classifier in the Feature Space

After extracting short isometric shapelet candidates, the next step is to select shapelets from these short isometric shapelet candidates. This subsection begins at the analysis of the selection of shapelets. Since it is the key point of substituting the ensemble classifier in the shapelet-dependent feature space.

As previously mentioned, in the process of selecting shapelets from shapelet candidates, if the prime information gain is used as the discrimination index of shapelet candidates, then the evaluation of a shapelet candidate can not get rid of searching a prime segmentation for data represented in a real number axis (see Subsection 2.1). And this operation is time-consuming.

On the other hand, the selected shapelets are also relevant to the distribution of transformed time series in the feature space. If nothing can be ensured of this distribution in the feature space, things become fairly complicated. The following illustration is shown to explain this point.

In the ensemble shapelet transform algorithm, the classifier is often an ensemble one of almost all kinds of typical classifiers trained in the feature space. It costs much time to train such an elaborate ensemble classifier. However, it is necessary to do that on account of the uncertainty of the distribution of data in the feature space. In that algorithm, each base classifier tries to catch one possible distribution of data in the feature space, while using the single classifier must undertake the risk of misestimating the data distribution. One radical cause of that plight is that the discrimination index of shapelets is designed without a thought about the combination of shapelets. That is to say, mere good separability in each dimension ensures little in the total space.

This illustration exemplifies that considering more than discrimination of a single shapelet is required while selecting shapelets from shapelet candidates. The combination of shapelets is another important issue while selecting shapelets. One example is that if the selected shapelet set constructing the feature space can ensure a high linear separability of the data distribution, the classification conducted in the feature space will become comparatively easy. In the Euclidean feature space constructed by the shapelet transform, each shapelet represents a dimension, and values in that dimension represent the distance to the shapelet. If projections of transformed data onto each dimension is completely separable, which means there is a cut line completely dividing data from different two classes, the transformed data can be surely linearly separable in the total space. However, in practice, the majority of axes is the one where the projection onto it can not be completely divided, even though shapelets are selected as discriminative as they can. Hence, the difficulty is to ensure a high degree of linear separability while projections of data onto a single axis can not be completely divided. Thanks to the next Proposition 2, this goal can be achieved by using the generalized Rayleigh quotient as the selection priority of shapelet candidates.

Before stating and proving Proposition 2, the generalized Rayleigh quotient used in this paper should be defined. For two different classes of data

distributed on a single real axis, the generalized Rayleigh quotient is calculated by the next formula:

$$GRQ(A, B) = \frac{|\mu(A) - \mu(B)|}{\sigma^2(A) + \sigma^2(B)} \quad (14)$$

where GRQ is a short hand of ‘generalized Rayleigh quotient’, $\mu(\cdot)$ is the function to get the mean value, and $\sigma^2(\cdot)$ is the function to get the variance. For the shapelet candidate in a binary TSC problem, after transforming the original time series to real numbers by distance calculation, Eq. (14) can be used to calculate the GRQ value.

The next part is the statement and the proof of the crucial Proposition.

Proposition 2 For a binary TSC problem in a Euclidean feature space constructed by the shapelet transform, the generalized Rayleigh quotient of the projections of transformed data onto any single axis has a positive correlation with the degree of the linear separability of the transformed data in the total space.

Proof Firstly, some notations are necessary:

$X \setminus Y \setminus X' \setminus Y'$: a real random vector
Ω	: set of all real random vectors
$\mu : \Omega \mapsto \cup_{k=1}^{\infty} R_k$: a function getting the mean vector of the random vector
$\mu_j : \Omega \mapsto R$: a function equals to $\pi_j \circ \mu$ where π_j is a projection map which gets the value of a vector's j -th dimension
$[]^2$: get a vector which the value of each dimension equals the square of the original value
$\sigma^2 : \Omega \mapsto \cup_{k=1}^{\infty} R_k$: a function getting the diagonal vector of the covariance matrix of the random vector
$\sigma_j^2 : \Omega \mapsto R$: a function equals to $\pi_j \circ \sigma^2$ where π_j is a projection map which gets the value of a vector's j -th dimension
$\Sigma_{X \setminus Y \setminus X' \setminus Y'}$: the covariance matrix of the random vector
LS	: the degree of the linear separability

of vectors of two different classes

Based on the above notations, the proof can start. Assume that there are two time series classes whose corresponding sets are A and B , a shapelet set C whose cardinality is k . A 's shapelet transform through C by some metric (see definition 1) forms the sample set of a k -dimensional real random vector X . The same process of B forms the sample set of a k -dimensional real random vector Y . By the central limit theorem, these two random vectors can be presumed to be independent spherical normally distributed. That is:

$$X \sim N(\mu(X), \Sigma_X) \quad (15)$$

$$Y \sim N(\mu(Y), \Sigma_Y) \quad (16)$$

And we naturally define the degree of the linear separability by the following formula:

$$LS = \max_{\mathbf{w}} P((X - Y) \cdot \mathbf{w} > 0) \quad (17)$$

$$\|\mathbf{w}\| = 1, \mathbf{w} \in R_k$$

For proving Proposition 2, we need to prove that $|\mu_j(X) - \mu_j(Y)|$ has a positive correlation with LS and $\sigma_j^2(X) + \sigma_j^2(Y)$ has a negative correlation with LS for any j in scope.

For a fixed \mathbf{w} , the following result can be deduced by the previous conditions.

$$(X - Y) \cdot \mathbf{w} \sim N((\mu(X) - \mu(Y)) \cdot \mathbf{w}, (\sigma^2(X) + \sigma^2(Y)) \cdot [\mathbf{w}]^2) \quad (18)$$

For the prime normal vector \mathbf{w} of Eq. (17), it has that:

$$(\mu(X) - \mu(Y)) \cdot \mathbf{w} \geq 0 \quad (19)$$

$$(\mu_j(X) - \mu_j(Y)) \cdot \mathbf{w}_j \geq 0 \quad 1 \leq j \leq k \quad (20)$$

For the first inequality, that is because \mathbf{w} can be substituted with $-\mathbf{w}$ if the inequality does not hold. Then $-\mathbf{w}$ is better than \mathbf{w} , which contradicts that \mathbf{w} is the prime normal vector. It is the same with the second inequality, if it is less than 0, just substitute \mathbf{w}_j with $-\mathbf{w}_j$ to get a better normal vector \mathbf{w}' . And it contradicts that \mathbf{w} is the prime normal vector. Fig. 5 shows these cases.

Assuming that the best LS and the prime normal vector \mathbf{w} have been acquired, if substitute X and Y with X' and Y' which are same with X and Y except for a specific j where $|\mu_j(X') - \mu_j(Y')| > |\mu_j(X) - \mu_j(Y)|$, then the following results hold from Eq. (18), (19) and (20).

$$\mu((X' - Y') \cdot \mathbf{w}') > \mu((X - Y) \cdot \mathbf{w}) \geq 0 \quad (21)$$

$$\sigma^2((X' - Y') \cdot \mathbf{w}') = \sigma^2((X - Y) \cdot \mathbf{w}) \quad (22)$$

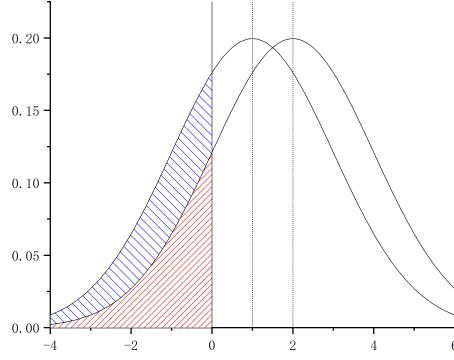


Fig. 5: Two independent normally distributed variables with the identical variance. The one whose mean is larger has a higher probability of being positive than the other. That's because the area under two curves are both 1 and the curve with the larger mean possesses a smaller area left to $x = 0$. Hence the curve with the larger mean has a larger area right to $x = 0$, which means a higher probability of getting a positive value.

Here \mathbf{w}' equals \mathbf{w} on all dimensions except for the j -th value. And $\mathbf{w}'_j = \text{sign}((\mu_j(X') - \mu_j(Y')) \cdot |\mathbf{w}_j|)$, which aims to make $(\mu_j(X') - \mu_j(Y')) \cdot \mathbf{w}'_j$ positive. Combining with (17), they shows that:

$$LS' \geq P((X' - Y') \cdot \mathbf{w}' > 0) > P((X - Y) \cdot \mathbf{w} > 0) = LS \quad (23)$$

Fig. 5 shows that situation. And this means that $|\mu_j(X) - \mu_j(Y)|$ has a positive correlation with LS for arbitrary j in scope.

Similarly, keep the assumption that the best LS and the prime normal vector \mathbf{w} of the optimization problem 17 have been acquired, and substitute X and Y with X' and Y' which are same with X and Y except for a specific j where $\sigma_j^2(X') + \sigma_j^2(Y') < \sigma_j^2(X) + \sigma_j^2(Y)$, then the following results hold from Eq. (18):

$$\mu((X' - Y') \cdot \mathbf{w}) = \mu((X' - Y') \cdot \mathbf{w}) \geq 0 \quad (24)$$

$$\sigma^2((X' - Y') \cdot \mathbf{w}) < \sigma^2((X - Y) \cdot \mathbf{w}) \quad (25)$$

Combining with (17), Eq. (23) holds too. Fig. 6 shows that situation. And this means that $\sigma_j^2(X) + \sigma_j^2(Y)$ has a negative correlation with LS for arbitrary j in scope. Then the proof of Proposition 2 is completed.

From the calculation formula of the GRQ (Eq. (14)), it can be seen that the GRQ surely has the ability to quantify the separation extent of data in a real number axis. Hence the large GRQ value guarantees the discrimination of a single selected shapelet. The prime information gain also has the ability.

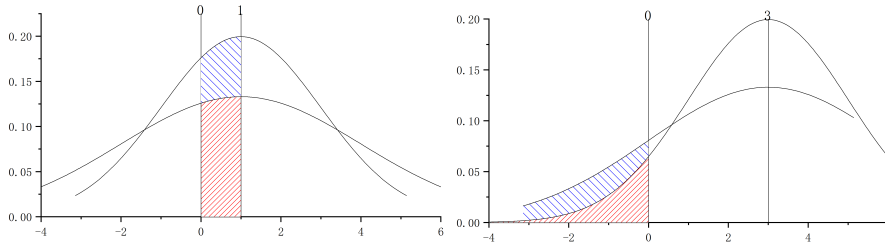


Fig. 6: For two independent normally distributed variables with the identical positive mean, the one whose variance is smaller has a higher probability of being positive than the other. There are two situations. The first one is that the left intersection point of two curves is left to $x = 0$, which is shown in the first picture. The second one is that the left intersection point of two curves is right to $x = 0$, which is shown in the second picture.

But the large GRQ value in each single axis can ensure a high degree of the linear separability in the total space, whereas the large prime information gain can not do that. And this advantage is exactly what Proposition 2 states. This property of the GRQ is the most important advantage of it compared with the prime information gain.

In Proposition 2, each axis of the feature space actually corresponds to the real number axis of a shapelet. And the projections of transformed time series onto each axis are actually the distances from time series to the corresponding shapelet. Hence, Proposition 2 can ensure a high degree of the linear separability of data in the feature space under the precondition of selecting shapelets with the large GRQ value. As a result, if shapelets are selected according to the rank of GRQ values, training a single SVM to classify data also works at most cases. Once the ensemble classifier is substituted with a single SVM, time consumption is largely reduced for the reduction of training costs. Moreover, using the GRQ as the selection priority of shapelet candidates also successfully gets rid of the time-consuming operation that searching the best segmentation for different data in a real number axis.

3.4 Outline and Time Complexity of Training SIST

Considering the small delay which may happen in time series, a small relaxation is added to Eq. (2):

$$\begin{aligned}
 & \text{Relaxed_Fixed_Dist}(\mathbf{s}, \mathbf{x}) = \\
 & \min \left\{ d(\mathbf{s}, P) \left| \begin{array}{l} P = (x_{i_1}, \dots, x_{i_k}), \\ i_1 < i_2 < \dots < i_k < j + k + r, \\ -l \leq i_1 - j \leq r, \\ 1 \leq i_1 \leq \text{Len}(\mathbf{x}) - k + 1 \end{array} \right. \right\} \quad (26)
 \end{aligned}$$

where both l and r are very small relaxation constants, P is the ordered subsequence which can be continuous or discontinuous, $Len(\cdot)$ is the function to get the length of time series, and other parameters are same with them in Eq. (2).

The algorithmic outline of training SIST is given in Algorithm 1.

Algorithm 1 Train the SIST classifier

Input: D the binary data set, L the shapelet length, r_a the left relaxation factor, r_b the right relaxation factor, N the number of shapelets
Output: Shapelet set S whose cardinality is N , a SVM classifier C with the linear kernel
 1: initialize a null set T ;
 2: **for** each time series $t \in D$ **do**
 3: initialize a L -length shapelet candidate set T_t by a L -length window sliding from the initial point to the end point of t with step length 1;
 4: $T = T \cup T_t$;
 5: **end for**
 6: initialize a priority queue S ;
 7: **for** each shapelet candidate $s \in T$ **do**
 8: **for** each time series $t \in D$ **do**
 9: calculate Relaxed Fixed Distance between s and t by Eq. (26);
 10: **end for**
 11: calculate the generalized Rayleigh quotient of the calculated distances by Eq. (14);
 12: set the generalized Rayleigh quotient as the priority of s ;
 13: $S = S \cup s$;
 14: **end for**
 15: S =subqueue of S from position 0 to $N - 1$
 16: do D 's shapelet transform through S by Relaxed Fixed Distance (the process is stated in definition 1) and get a vector set Ω ;
 17: train a SVM C with linear kernel in Ω ;

For a data set D of n time series of length m , fixing the length of shapelet candidates at k , the time consumption of training SIST can be estimated as follows:

$$\begin{aligned}
 T(SIST) &= \mathcal{O}(n(m - k + 1)T(SP) + T(R) + T(SVM)) \\
 &\approx \mathcal{O}(n^2mk + nm \log(nm) + Nn^2) \\
 &= \mathcal{O}(n^2 \max(mk, N)) \\
 &< \mathcal{O}(n^2m^2)
 \end{aligned} \tag{27}$$

where $T(SP)$, which is multiplied by the number of shapelet candidates, means the time complexity of calculating the selection priority of shapelet candidates, $T(R)$ means the time complexity of ranking all the shapelet candidates, and $T(SVM)$ means the time complexity of training a SVM with the linear kernel in the feature space. Since the components of transformed vectors can be acquired in the process of calculating the selection priority, there is no extra time needed for the shapelet transform based on the selected shapelet basis. Empirically, N , which is the dimension of the feature space, is set less than m^2 . And k is obviously less than m . Therefore, the inequality is satisfied. And

Table 1: Hyperparameter Set

delete overlap shapelet	true, false
shapelet length	3,4
left and right relaxation factor	3,4
shapelet number	10,50,100,250,500,750, 1000,1250,1500,2000

in the ensemble ST algorithm, the time complexity is $\mathcal{O}(n^2m^4)$ [25; 8]. This time complexity analysis shows some advantages of the proposed strategies. And in the next section, some experimental evidences of the advantages are given.

4 Experimental Evidences

4.1 Compared Algorithms and Datasets

To show the advantages of the proposed strategies, SIST is compared with the state-of-the-art. According to the research of A. Bagnall et al.[3], the following eight algorithms are the state-of-the-art algorithms. They are COTE (Collection of Transformation Ensembles) [2], ST (ensemble edition) [8], BOSS (Bag of SFA Symbols, ensemble edition) [41], EE (Elastic Ensemble) [33], DTWF (Dynamic Time Warping Features) [28], TSF (Time Series Forest) [18], TSBF (Time Series Bag of Features) [7], and LPS (Learned Pattern Similarity) [6].

The proposed algorithm has some hyperparameters to be selected, and Table 1 shows the hyperparameter sets used in the experiments. Line 1 is about whether removing the overlap shapelets. The item ‘true’ means that if two shapelets overlap, then the one with the lower selection priority is removed. And this choice may make the final shapelet number smaller than the target number. This item means each discriminative position in a time series is at most once selected for classification. It is to say, users want a balance among every discriminative position’s contribution to classification in case that one position’s information covers others. The choice ‘false’ is just the opposite, which means users want to see that the more discriminative the position is, the stronger effects it has on the classification. Line 2 is about the length of shapelet candidates. Hyperparameters in line 3 decide the relaxation extent of the Fixed Distance calculation. Line 4 is about the number of shapelets used for the shapelet transform.

As for data sets, only the binary data sets from UCI data sets are selected, since Eq. (14) is restricted on binary TSC problems. In principle, for a multiclass TSC problem, the ‘one vs all’ strategy can solve it. However, the time complexity will be multiplied by the number of classes under this strat-

Table 2: Data Attributes and Hyperparameters Chosen by 10-fold Cross Validation. DO:Delete Overlap. SL: Shapelet Length. Relaxation Factor: RF. Shapelet Number: SN. PPOC: ProximalPhalanxOutlineCorrect.

Data Attribute			Hyperparameter of SIST			
Dataset	Train\Test	Length	DO	SL	L\R RF	SN
Coffee	28\28	286	true	3	3\3	10
DistalPhalanxOutlineCorrect	600\276	80	true	4	4\4	2000
Earthquakes	322\139	512	true	3	3\3	10
ECG200	100\100	96	true	3	4\3	1500
ECGFiveDays	23\861	136	false	3	3\3	2000
GunPoint	50\150	150	false	4	3\3	1250
Ham	109\105	431	true	3	4\3	50
Herring	64\64	512	true	4	4\3	10
ItalyPowerDemand	67\1029	24	false	3	4\4	100
MiddlePhalanxOutlineCorrect	600\291	80	true	3	4\4	1500
MoteStrain	20\1252	84	true	4	3\4	250
PPOC	600\291	80	true	4	3\3	2000
SonyAIBORobotSurface1	20\601	70	false	4	4\3	50
SonyAIBORobotSurface2	27\953	65	false	3	3\3	2000
Strawberry	613\370	235	false	4	4\4	1250
TwoLeadECG	23\1139	82	true	3	4\3	50
Wine	57\54	234	true	3	3\3	250

egy. Hence, the ‘one vs all’ strategy may be not a good method for using the proposed strategies in a multiclass TSC problem. Multiclass TSC problems have a different structure from binary TSC problems, and this is another issue needing to be explored rather than tackled by a simple ‘one vs all’ strategy. Actually, the future work is regarding to expanding the proposed strategies to multiclass TSC problems. But this paper mainly focuses on the theoretical evidences and some advantages of the proposed strategies. Table 2 shows details of data sets and hyperparameter selections of SIST. Since these data sets are commonly used benchmark data sets in the research area of TSC, the default training/testing split settings are used here for a fair comparison.

Table 3: Accuracy Comparison on Binary Datasets with eight Top TSC Algorithms. DPOC: DistalPhalanxOutlineCorrect. ECGFD: ECGFiveDays. IPD: ItalyPowerDemand. MPOC: MiddlePhalanxOutlineCorrect. PPOC: ProximalPhalanxOutlineCorrect SAIBORS1: SonyAIBORobotSurface1. SAIBORS2: SonyAIBORobotSurface2. TLECG: TwoLeadECG.

Dataset	DTWF	ST	BOSS	TSF	TSBF	LPS	EE	COTE	SIST
Coffee	0.973	0.995	0.989	0.989	0.982	0.95	0.989	1.000	1.000
DPOC	0.796	0.829	0.815	0.810	0.816	0.767	0.768	0.804	0.830
Earthquakes	0.748	0.737	0.746	0.747	0.757	0.668	0.735	0.747	0.871
ECG200	0.819	0.840	0.891	0.868	0.847	0.808	0.881	0.873	0.86
ECGFD	0.907	0.955	0.983	0.922	0.849	0.840	0.847	0.986	0.978
GunPoint	0.964	0.999	0.994	0.961	0.965	0.972	0.974	0.992	0.967
Ham	0.795	0.808	0.836	0.795	0.711	0.685	0.763	0.805	0.838
Herring	0.609	0.653	0.605	0.606	0.591	0.549	0.566	0.632	0.875
IPD	0.948	0.953	0.866	0.958	0.926	0.914	0.914	0.970	0.978
MPOC	0.798	0.815	0.808	0.794	0.800	0.770	0.782	0.801	0.897
MoteStrain	0.891	0.882	0.846	0.874	0.886	0.917	0.875	0.902	0.889
PPOC	0.829	0.881	0.867	0.847	0.861	0.851	0.839	0.871	0.900
SAIBORS1	0.884	0.888	0.897	0.845	0.839	0.842	0.794	0.899	0.839
SAIBORS2	0.859	0.924	0.889	0.856	0.825	0.851	0.870	0.960	0.877
Strawberry	0.970	0.968	0.970	0.963	0.968	0.963	0.959	0.963	0.959
TLECG	0.958	0.984	0.985	0.842	0.910	0.928	0.959	0.983	0.982
Wine	0.892	0.926	0.912	0.881	0.879	0.884	0.887	0.904	1.000

4.2 Comparison Experiments

This subsection will show advantages of the proposed strategies by comparing SIST with the state-of-the-art algorithms in terms of accuracy and efficiency. The purpose of the proposed strategies is to reduce the time complexity with little loss of the accuracy achieved by the state-of-the-art on binary TSC problems. Hence, it should be checked that SIST indeed achieves a top classification accuracy on most of binary TSC problems.

Table 3 presents the accuracy comparison between SIST and the state-of-the-art algorithms on many data sets. The accuracy of the compared algorithms comes from the TSC community. The hyperparameters of these compared algorithms were strictly selected to achieve as high accuracy as possible.

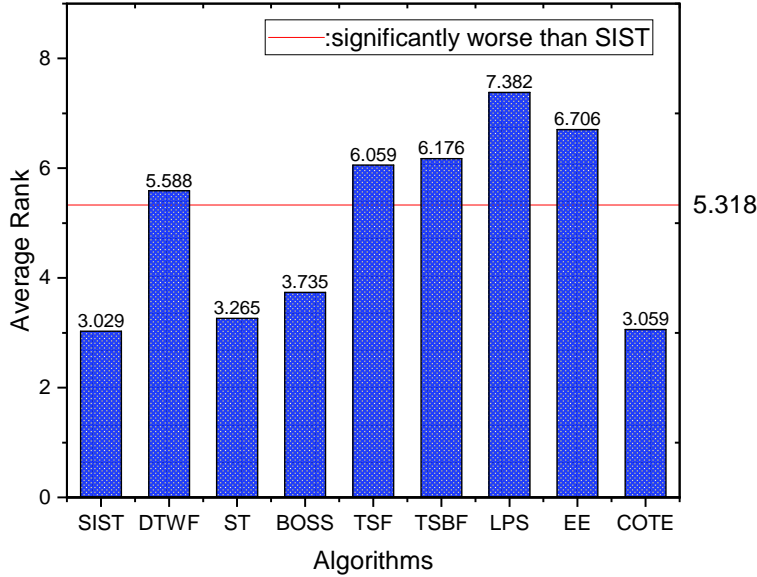


Fig. 7: Average accuracy rank and Friedman test with 95% confidence. The average rank in this figure is the arithmetic mean of the accuracy ranks on all the experimental data sets. The red cut line in this figure is the threshold calculated by the Friedman test.

According to the table, SIST performs best on more than a half of the data sets. On the other half of the experimental data sets, SIST may not be the best one, but it still possesses a reasonable accuracy compared with the state-of-the-art algorithms. As it is previously mentioned, the model proposed in the paper tries to reduce the time complexity with the cost of as small accuracy drop as possible. The strategies exploited in SIST mainly serve the purpose of nearly losslessly reducing the time complexity, and from the theoretical analysis in the paper, it is also clear that the strategies here will not manifestly boost the classification performance on the basis of the state-of-the-art algorithms. Hence, it is sensible here that SIST does not prevail in all the datasets. The key point here is to check whether SIST also performs well in the datasets where it does not achieve the best accuracy. Actually, from the result in the table, the accuracy of SIST is fairly close to the state-of-the-art accuracy on these data sets. The experimental result here along with the theoretical analysis in Section 3 shows that SIST does achieve the purpose of keeping accurate enough.

More details about the accuracy comparison can be seen in Fig. 7. In this figure, all the algorithms' average ranks are depicted. By putting these average

ranks in the same histogram, a holistic view of the comparison is illustrated between SIST and the compared algorithms. According to the data in this figure, it can be judged whether SIST is significantly better than the compared algorithms by the Friedman test with a 95% confidence. The red cut line in the figure is a threshold calculated according to the Friedman test. SIST are significantly better than an compared algorithm if its average rank is larger than the threshold. In Fig. 7, the red cut line goes across the bars of the DTWF, the TSF, the TSBF, the LPS, and the EE, which means average ranks of those five algorithms are larger than the threshold. Hence, SIST are significantly better than those five algorithms in terms of classification accuracy. The four remainder algorithms are the ST, the BOSS, the COTE, and SIST. And they are in the same level in terms of the classification accuracy. Although SIST is not significantly better than the ST, the BOSS, and the COTE in the Friedman test with a 95% confidence, the average rank of SIST is still smaller than the average ranks of those three algorithms. Hence, SIST is at least not worse than the ST, the BOSS, and the COTE in terms of the classification accuracy.

Based on the above experimental evidences and analysis, the ST, the BOSS, the COTE, and SIST can be presently regarded as the first tier candidates of the TSC algorithms in terms of the classification accuracy. Next, the efficiency comparison among the first-tier algorithms will be focused on. Since the purpose of the proposed strategies is to reduce the time complexity with little loss of the accuracy achieved by the state-of-the-art, the precondition of keeping the good accuracy is important. Therefore, these algorithms that may possess the lower time consumption are not considered since they can not keep a high accuracy. In other words, the efficiency comparison focuses only on the first-tier candidates.

Table 4 presents the time consumption comparison on all the experimental data sets in the same environment. Since these four algorithms are all eager learning algorithms, the time consumption is mainly spent in training the classifier. Hence, the time shown in Table 4 is the training time. From Table 4, it can be seen that SIST has the lowest time consumption on all the experimental data sets. SIST has evident advantage compared with the ST, the BOSS, and the COTE in terms of time consumption, which indicates the running time advantage. The COTE has a fairly large training time although it is hot on the heels of SIST in Fig. 7. To some extent, the huge training time of the COTE makes some troubles in the practical application. On some data sets, the training time of the COTE is several days, whereas SIST only spend some minutes in getting a similar classification result. On some data sets, the training time of the compared first-tier algorithms may be some hours or some minutes, whereas SIST only spends some seconds. On some small-scale datasets such as ‘ECG200’, ‘ECGFiveDays’, and ‘ItalyPowerDemand’, the BOSS algorithm performs competitively compared with SIST. However, as the scale of datasets increases, the time consumption of the BOSS algorithm swells much faster than SIST. For instance, on some large-scale datasets, such as ‘Ham’, ‘Herring’, and ‘Earthquakes’, SIST performs more efficiently than the BOSS algorithm. The rationale behind it is that the BOSS algorithm exploits two technologies, called

Table 4: Time Comparison on Binary Datasets among the first-tier Algorithms with the Same Accuracy Level (CPU : Intel(R) Core(TM) i7-6500U CPU @ 2.50GHz ; RAM : 8GB ; Operating System : Windows 10 x64)

DataSet	ST	BOSS	COTE	SIST
Coffee	6.3s	6.6s	9.5E+03s	0.8s
DistalPhalanxOutlineCorrect	9.5E+03s	91.8s	2.9E+05s	88.9s
Earthquakes	1.5E+03s	1.6E+03s	9.1E+05s	61.3s
ECG200	64.5s	5.0s	1.3E+04s	1.5s
ECGFiveDays	7.6s	1.1s	1.1E+03s	0.3s
GunPoint	16.2s	3.4s	7.0E+03s	0.9s
Ham	51.1s	133.7s	2.8E+05s	6.4s
Herring	15.3s	66.2s	1.8E+05s	5.4s
ItalyPowerDemand	16.7s	0.6s	88.3s	0.1s
MiddlePhalanxOutlineCorrect	1.3E+05s	101.5s	2.5E+05s	34.1s
MoteStrain	4.7s	0.5s	151.8s	0.1s
ProximalPhalanxOutlineCorrect	9.8E+03s	78.3s	2.6E+05s	50s
SonyAIBORobotSurface1	2.0s	0.5s	114.2	0.1s
SonyAIBORobotSurface2	4.6s	1.0s	212.8s	0.2s
Strawberry	1.0E+04s	790.5s	5.3E+05s	279.7s
TwoLeadECG	4.4s	0.6s	283.0s	0.1s
Wine	11.2s	9.0s	4.3E+04s	0.6s

Discrete Fourier Transform (DFT) and Multiple Coefficient Binning (MCB) [41]. The running time of these two technologies is sensitive to the scale of the training data. Therefore, the efficiency advantage of SIST compared with the BOSS algorithm becomes increasingly evident when the scale of the training data grows large. In summary, from the results in Table 4, SIST outperforms the four first-tier algorithms in terms of the running time, which implies the effectiveness of the proposed strategies.

Next, a further comparison about the efficiency is conducted. By defining the product of the train set size and the data length as the scale of a data set, the experimental data sets are sorted into three categories according to their scales. Then the average accuracy and the average training time of these four compared algorithms are depicted in the coordinate system. Fig. 8 illustrates the results where three kinds of data sets correspond to three graphs. The vertical axis represents the average accuracy and the horizontal axis represents

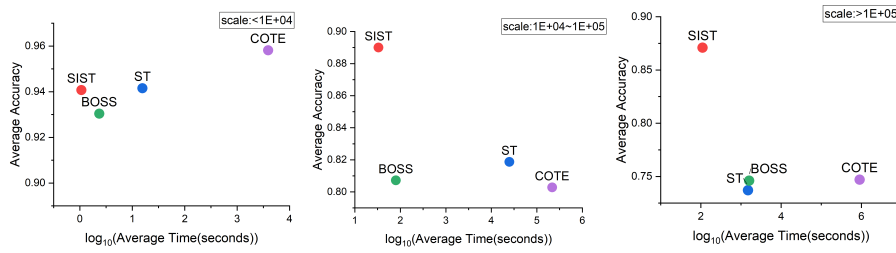


Fig. 8: Time-Accuracy comparison on data sets of different scale (scale is the product of train set size and data length)

the average training time. Note that the average training time is dealt with a logarithmic function basing 10 since the difference of the average training time is too big to depict them in a coordinate system. Hence, the horizontal distance is not uniform or even. The real time difference increases exponentially as the horizontal distance grows linearly in the coordinate system.

Firstly, the average accuracy of all the compared algorithms declines as the scale of data sets inclines. Secondly, no matter what the scales of data sets are, SIST remains the lowest average training time while the COTE algorithm has the highest one. Thirdly, on the data sets with a scale more than $1E+04$, SIST achieves the best average accuracy as well as the lowest average training time. Fourthly, as the scale of data sets increases, it is increasingly obvious of both the time advantage and the accuracy advantage of SIST. Fifthly, there is no algorithm dominating SIST in Fig. 8.

According to those discoveries in Table 4 and Fig. 8, SIST indeed possesses an efficiency advantage on binary TSC problems. The superiority of SIST are supported by the two proposed strategies.

Besides the state-of-the-art algorithms, SIST is compared with other shapelet-based time reduction algorithms in the research field of TSC. They include LS (Learning Time-series Shapelets) [23], EL (Efficient Learning of Time-series Shapelets)[26], and FS (Fast Shapelets) [29]. For a fair comparison, we keep the default hyperparameter settings in their papers and use the code they offer to the public. The result is shown in Table 5. From the table, we observe that EL is the most efficient algorithm and SIST is the most accurate algorithm. LS has a reasonable accuracy but a comparatively poor efficiency, and the FS reverses the situation in the LS. On some data sets, SIST does not achieve the best accuracy, but it still possesses a fairly well accuracy close to the best accuracy. Though SIST is not as efficient as the EL, the running time of it is also acceptable in most cases. EL is based on a gradient method. It formulates the shapelet extraction problem as an optimization problem, but the weakness is that the optimization problem is not convex due to the nonlinear constraint. Therefore, it may have the overfitting problem or even the divergent problem, which leads to unsteady classification performance. For instance, on the data set 'Wine', both two gradient methods diverge, the performance of both EL

Table 5: The performance of SIST compared with LS, EL, and FS(CPU : Intel(R) Core(TM) i7-6500U CPU @ 2.50GHz ; RAM : 8GB ; Operating System : Windows 10 x64). DPOC: DistalPhalanxOutlineCorrect. ECGFD: ECGFiveDays. IPD: ItalyPowerDemand. MPOC: MiddlePhalanxOutlineCorrect. PPOC: ProximalPhalanxOutlineCorrect SAIBORS1: SonyAIBORobotSurface1. SAIBORS2: SonyAIBORobotSurface2. TLECG: TwoLeadECG.

Accuracy/Time(s)	LS	EL	FS	SIST
Coffee	1.000(1)/77.6(4)	1.000(1)/0.4(1)	0.964(4)/5.3(3)	1.000(1)/0.8(2)
DPOC	0.741(2)/305.9(4)	0.713(4)/0.4(1)	0.728(3)/18.6(2)	0.830(1)/88.9(3)
Earthquakes	0.748(2)/4.7E+03(4)	0.711(4)/3.6(1)	0.712(3)/1.1E+03(3)	0.871(1)/61.3(2)
ECG200	0.850(2)/57.9(4)	0.84(3)/0.1(1)	0.75(4)/2.3(3)	0.86(1)/1.5(2)
ECGFD	1.000(1)/16.5(4)	0.920(4)/0.1(1)	0.995(2)/0.7(3)	0.978(3)/0.3(2)
GunPoint	1.000(1)/49.3(4)	0.967(2)/0.1(1)	0.94(4)/1.4(3)	0.967(2)/0.9(2)
Ham	0.686(2)/1.0E+03(4)	0.600(4)/1.1(1)	0.667(3)/157.8(3)	0.838(1)/6.4(2)
Herring	0.609(3)/763.1(4)	0.641(2)/4.2(1)	0.609(3)/91.2(3)	0.875(1)/5.4(2)
IPD	0.962(2)/5.2(4)	0.946(3)/0.1(1)	0.906(4)/0.1(1)	0.978(1)/0.1(1)
MPOC	0.780(2)/323.3(4)	0.750(3)/0.7(1)	0.663(4)/15.1(2)	0.897(1)/34.1(3)
MoteStrain	0.913(1)/6.5(4)	0.888(3)/0.1(1)	0.798(4)/0.2(3)	0.889(2)/0.1(1)
PPOC	0.767(3)/303.1(4)	0.738(4)/2.2(1)	0.838(2)/11.7(2)	0.900(1)/50.0(3)
SAIBORS1	0.952(1)/4.7(4)	0.929(2)/0.1(1)	0.686(4)/0.2(3)	0.839(3)/0.1(1)
SAIBORS2	0.890(1)/6.4(4)	0.749(4)/0.1(1)	0.790(3)/0.2(2)	0.877(2)/0.2(2)
Strawberry	0.884(4)/2.2E+03(4)	0.941(2)/0.7(1)	0.908(3)/77.8(2)	0.959(1)/279.7(3)
TLECG	1.000(1)/7.2(4)	0.990(2)/0.1(1)	0.946(4)/0.2(3)	0.982(3)/0.1(1)
Wine	0.500(4)/144.0(4)	0.537(3)/0.3(1)	0.778(2)/4.7(3)	1.000(1)/0.6(2)

and LS is not good. While the running time of SIST is slightly longer than EL, but its accuracy is much better than EL. From a holistic view, SIST has the steadiest and possibly the most accurate classification performance in the experiments.

4.3 Hyperparameter Analysis

There are four types of hyperparameters in SIST. To study their respective influence on the result, we fix other three types of hyperparameters when studying one type of them. For instance, if the hyperparameter ‘shapelet length’ is

studied, then there are $2 \times 4 \times 10 = 80$ possible combinations of other three types of hyperparameters 1. For each possible combination, we consider all the possible choices of the ‘shapelet length’ and get the classification accuracy of each choice with the fixed three other hyperparameters. Then, a group of classification accuracy is obtained on each data set for each combination of other three hyperparameters, and the standard deviation of the group of classification accuracy is calculated. Therefore, for each data set and each possible combination of other three hyperparameters, a standard deviation is reported to show the sensitivity of SIST on that data set to the hyperparameter ‘shapelet length’. An overall result is depicted in the above line charts. In the line chart, each polyline represents a data set, and each point in the polyline is the sensitive extent of SIST to the relative hyperparameter on the data set under a specific setting of other three hyperparameters. The sensitivity is the standard deviation calculated according to the rule described above.

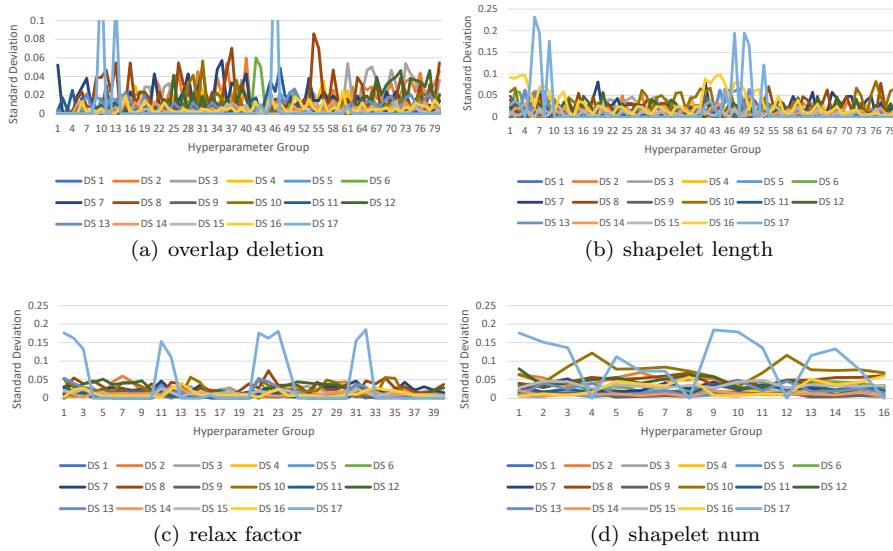


Fig. 9: Hyperparameter analysis

At first glance, the overall results are haphazard. But in fact, some observations can be found. Firstly, the sensitivity of SIST to hyperparameters differs on different data sets. Secondly, the sensitivity of SIST to one type of hyperparameter is strongly affected by the setting of other three types of hyperparameters. Thirdly, the rank of the sensitivity of SIST to the four types of hyperparameters may also differ on different data sets. Note that the third discovery is different from the first discovery. The first result indicates that the property of data sets has influences on the sensitivity of SIST to the four types of hyperparameters, and the third result indicates that the influences of data

sets on the sensitivity of SIST to hyperparameters are not even or consistent on the four types of hyperparameters.

From the above observation, the sensitivity of SIST to a single type of hyperparameter is affected by both the data set and the setting of other three types of hyperparameters. Now, we analyze the influences of the hyperparameter from a higher perspective. We try discarding the factor of the data set and the other types of hyperparameters and exploring the overall sensitivity of SIST to each type of hyperparameters. For each type of hyperparameter, we count the relative frequency of the standard deviation larger than some threshold in Figure 9. For instance, for the hyperparameter ‘shapelet length’, there are 17 data sets and 80 groups of settings of other three types of hyperparameters. Therefore, there are $17 \times 80 = 1360$ standard deviation points. Then, for each threshold, we count the proportion of the points larger than the threshold in all the 1360 points. Finally, we plot each proportion together in a polyline. The result is shown in the following figure.

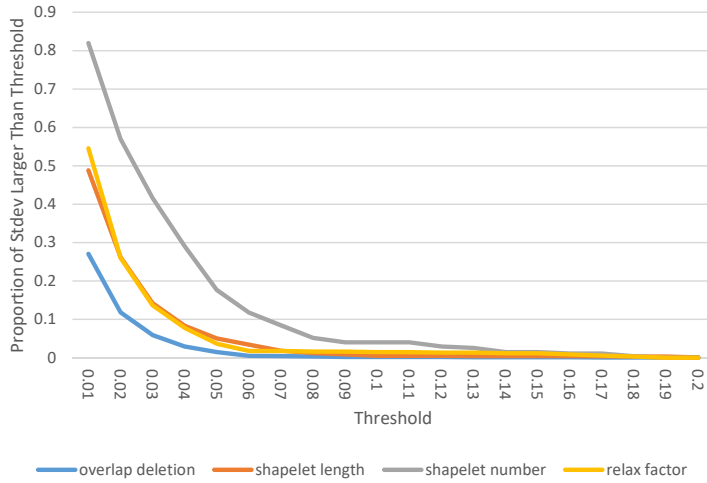


Fig. 10: The sensitivity of the SIST to the four types of hyperparameters

The result in Figure 10 indicates that SIST is the most sensitive to ‘shapelet number’ in the four types of hyperparameters, and the most insensitive one is ‘overlap deletion’. For one type of hyperparameter, we can roughly regard the standard deviation as an average fluctuation range of the accuracy of SIST on different choices of the type of hyperparameter. Then some information can be derived from some key points in the figure. The data located at 0.05 on the Threshold axis show that there are nearly less than 5% cases with an accuracy fluctuation range larger than 5% when the changing hyperparameter is ‘overlap deletion’, ‘shapelet length’, or ‘relax factor’. The data located at 0.1 on the Threshold axis show that there are almost no cases with an accuracy fluctuation range larger than 10% when the changing hyperparameter is

‘overlap deletion’, ‘shapelet length’, or ‘relax factor’. Therefore, the influence of the hyperparameter ‘shapelet number’ on SIST may be stronger than other three types of hyperparameters.

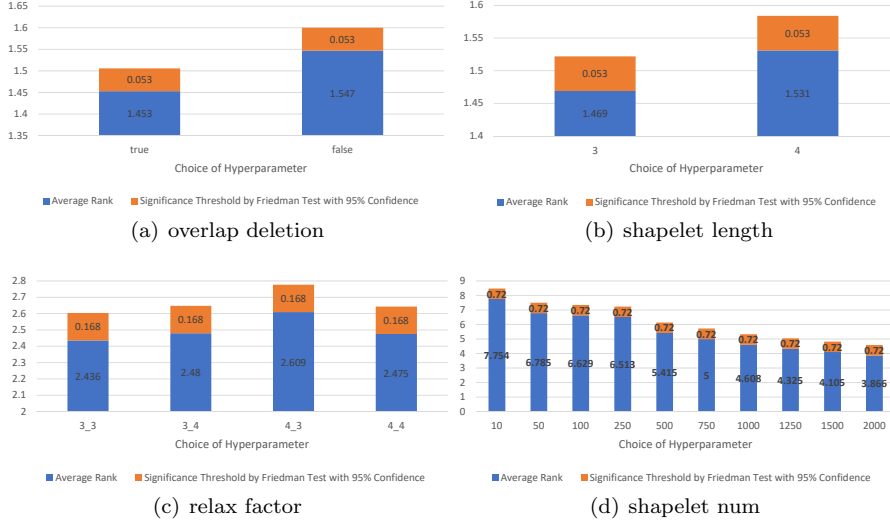


Fig. 11: The Friedman test for the preference of the choices of hyperparameters

Another observation is about the preference of SIST to some choices of each type of hyperparameter. We carry out the comparison experiment on each choice for each type of hyperparameter. For instance, for the hyperparameter ‘shapelet number’, there are 17 data sets and $2 \times 2 \times 4 = 16$ settings of other three types of hyperparameters. Therefore, there are $17 \times 16 = 272$ cases; For each case, there are 10 choices of the ‘shapelet number’, and we can get the accuracy for each choice. By ranking these accuracies, we can further get a rank of each choice in each case. Finally, we calculate the average rank of each choice on all the 272 cases and depict it in Figure 11. We check the significance of the preference of SIST on some choices by the Friedman test with a 95% confidence. Then we can check the preference of SIST on any pair of choices of one type of hyperparameter by comparing the difference of their average ranks with the corresponding Friedman threshold. Some obvious results are concluded as follows. On the hyperparameter ‘overlap deletion’, SIST prefers ‘deleting overlap shapelets’ to ‘not deleting overlap shapelets’; On the hyperparameter ‘shapelet length’, SIST prefers ‘shapelet length 3’ to ‘shapelet length 4’; On the hyperparameter ‘relax factor’, SIST prefers ‘3’3’, ‘3’4’, and ‘4’4’ to ‘4’3’ (here, ‘ a ’ b ’ means that setting left relax factor as a and right relax factor as b in the calculation of the Relaxed Fixed Distance.), and there is no significant preference among ‘3’3’, ‘3’4’, and ‘4’4’, and there is also no significant preference among ‘3’4’, ‘4’3’, and ‘4’4’. On the hyperparameter

‘shapelet number’, the situation is a little complex since there are 10 choices of the hyperparameter, but one can easily check the preference of SIST on any pair of two choices. A manifest result is that SIST may prefer more shapelets in general. However, please note that these results are derived in an overall view, and when it comes to some specific data set and hyperparameter setting, the results may not hold.

4.4 Ablation Experiments

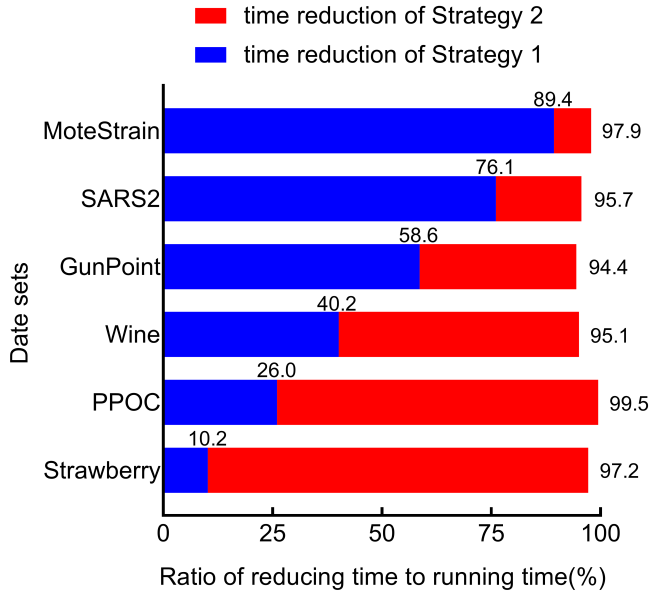


Fig. 12: Ablation experiments. The amount of the total bar is the proportion of the total saving time in the running time of the ensemble ST. The blue bar corresponds to the proportion of the saving time in the first period while the red bar corresponds to the saving time in the second period. SARS2: SonyAIBORobotSurface2. PPOC: ProximalPhalanxOutlineCorrect.

To further verify the contribution of each strategy on time reduction, ablation experiments are carried out on some data sets, and the results are depicted in Figure 12. As previously mentioned, the two proposed strategies are used to reduce the time complexity of the ensemble ST algorithm. The first strategy embodies its efficiency in the shapelet extraction and feature space construction period. The second strategy takes effect in the classifier training

period. And the two periods exactly compose the whole training process of the ST algorithm. Here, the running time of the ensemble ST on each strategy is compared with SIST to indicate the effectiveness of the other strategy.

For different data sets, the absolute quantity of time reduction may differ in magnitude. Hence, the relative quantity of time reduction is used in the result for more convenient comparison. In Figure 12, the amount of the total bar is the proportion of the total saving time in the running time of the ensemble ST. The blue bar corresponds to the proportion of the saving time in the first period while the red bar corresponds to the saving time in the second period. The data sets in this figure are arranged in the order of their scales. From the results, it is apparent that the two strategies are powerful in reducing the running time, since they together reduce 94.4% ~ 99.5% running time of the ensemble ST on each data set. As the scale of the data set increases, Strategy 2 contributes more to time reduction than Strategy 1. Therefore, in the small scale data sets, Strategy 1 plays a major role in time reduction, whereas Strategy 2 is the key to time reduction in the large scale data sets. And when the data set is in a middle scale, the contributions of these two strategies are approximately the same.

5 Conclusion and Future Work

In this paper, we have proposed an novel algorithm, short isometric shapelet transform (SIST), to solve the high time complexity problem of the ensemble shapelet transform algorithm. Two strategies applied in SIST have been guaranteed by the theoretical evidences that shows SIST reduces the time complexity with the near-lossless accuracy. Furthermore, the empirical experiments demonstrate the effectiveness of the proposed algorithm. Supported by the theoretical evidences, the two strategies adopted by SIST actually have generality in algorithms based on the shapelet transform. Hence, the future work is trying to apply these two strategies to more scenarios such as multi-class classification [35], semi-supervised learning and so forth. In the future, theoretical evidences will also be further explored to improve the theory of these two strategies in SIST.

References

1. Apostolico A, Bock ME, Lonardi S (2002) Monotony of surprise and large-scale quest for unusual words. *Journal of computational molecular cell biology* 10 3-4:283–311
2. Bagnall A, Lines J, Hills J, Bostrom A (2015) Time-series classification with cote: The collective of transformation-based ensembles. *IEEE Transactions on Knowledge and Data Engineering* 27:2522–2535
3. Bagnall A, Lines J, Bostrom A, Large J, Keogh EJ (2016) The great time series classification bake off: a review and experimental evaluation of recent algorithmic advances. *Data Mining and Knowledge Discovery* 31:606–660

4. Bagnall AJ, Janacek GJ (2014) A run length transformation for discriminating between auto regressive time series. *J Classification* 31:154–178
5. Batista GEAPA, Keogh EJ, Tataw OM, de Souza VMA (2013) Cid: an efficient complexity-invariant distance for time series. *Data Mining and Knowledge Discovery* 28:634–669
6. Baydogan MG, Runger GC (2015) Time series representation and similarity based on local autopatterns. *Data Mining and Knowledge Discovery* 30:476–509
7. Baydogan MG, Runger GC, Tuv E (2013) A bag-of-features framework to classify time series. *IEEE Transactions on Pattern Analysis and Machine Intelligence* 35:2796–2802
8. Bostrom A, Bagnall A (2015) Binary shapelet transform for multiclass time series classification. *T Large-Scale Data- and Knowledge-Centered Systems* 32:24–46
9. Bostrom A, Bagnall A, Lines J (2016) Evaluating improvements to the shapelet transform
10. Chen H, Yao X (2009) Regularized negative correlation learning for neural network ensembles. *IEEE Transactions on Neural Networks* 20(12):1962–1979
11. Chen H, Yao X (2010) Multiobjective neural network ensembles based on regularized negative correlation learning. *IEEE Transactions on Knowledge and Data Engineering* 22(12):1738–1751
12. Chen H, Tiño P, Yao X (2009) Predictive ensemble pruning by expectation propagation. *IEEE Transactions on Knowledge and Data Engineering* 21(7):999–1013
13. Chen H, Tang F, Tino P, Yao X (2013) Model-based kernel for efficient time series analysis. In: *Proceedings of the 19th ACM SIGKDD international conference on Knowledge discovery and data mining*, pp 392–400
14. Chen H, Tiño P, Rodan A, Yao X (2013) Learning in the model space for cognitive fault diagnosis. *IEEE Transactions on Neural Networks and Learning Systems* 25(1):124–136
15. Chen H, Tiño P, Yao X (2014) Cognitive fault diagnosis in tennessee eastman process using learning in the model space. *Computers & Chemical Engineering* 67:33–42
16. Chen H, Tang F, Tino P, Cohn AG, Yao X (2015) Model metric co-learning for time series classification. In: *Twenty-Fourth International Joint Conference on Artificial Intelligence*, pp 3387–3394
17. Corduas M, Piccolo D (2013) Clustering and classification by the autoregressive metric
18. Deng H, Runger GC, Tuv E, Martyanov V (2013) A time series forest for classification and feature extraction. *Inf Sci* 239:142–153
19. Gionis A, Mannila H (2003) Finding recurrent sources in sequences. In: *RECOMB*
20. Gong Z, Chen H (2018) Sequential data classification by dynamic state warping. *Knowledge and Information Systems* 57(3):545–570

21. Górecki T, Luczak M (2012) Using derivatives in time series classification. *Data Mining and Knowledge Discovery* 26:310–331
22. Górecki T, Luczak M (2014) Non-isometric transforms in time series classification using dtw. *Knowl-Based Syst* 61:98–108
23. Grabocka J, Schilling N, Wistuba M, Schmidt-Thieme L (2014) Learning time-series shapelets. In: *KDD*
24. Guido RC (2018) Fusing time, frequency and shape-related information: Introduction to the discrete shapelet transform’s second generation (dst-ii). *Information Fusion* 41:9–15
25. Hills J, Lines J, Baranauskas E, Mapp J, Bagnall A (2013) Classification of time series by shapelet transformation. *Data Mining and Knowledge Discovery* 28:851–881
26. Hou L, Kwok JT, Zurada JM (2016) Efficient learning of timeseries shapelets. In: *AAAI*
27. Jeong Y, Jeong MK, Omitaomu OA (2011) Weighted dynamic time warping for time series classification. *Pattern Recognition* 44:2231–2240
28. Kate RJ (2015) Using dynamic time warping distances as features for improved time series classification. *Data Mining and Knowledge Discovery* 30:283–312
29. Keogh EJ, Rakthanmanon T (2013) Fast shapelets: A scalable algorithm for discovering time series shapelets. In: *SDM*
30. Li Y, Hong J, Chen H (2019) Short sequence classification through discriminable linear dynamical system. *IEEE Transactions on Neural Networks and Learning Systems* 30(11):3396–3408
31. Lin J, Keogh EJ, Wei L, Lonardi S (2007) Experiencing sax: a novel symbolic representation of time series. *Data Mining and Knowledge Discovery* 15:107–144
32. Lin J, Khade R, Li Y (2012) Rotation-invariant similarity in time series using bag-of-patterns representation. *Journal of Intelligent Information Systems* 39:287–315
33. Lines J, Bagnall A (2014) Time series classification with ensembles of elastic distance measures. *Data Mining and Knowledge Discovery* 29:565–592
34. Lines J, Taylor S, Bagnall A (2016) Hive-cote: The hierarchical vote collective of transformation-based ensembles for time series classification. 2016 IEEE 16th International Conference on Data Mining (ICDM) pp 1041–1046
35. Lyu S, Tian X, Li Y, Jiang B, Chen H (2019) Multiclass probabilistic classification vector machine. *IEEE Transactions on Neural Networks and Learning Systems* pp 1–14
36. Marteau PF (2009) Time warp edit distance with stiffness adjustment for time series matching. *IEEE Transactions on Pattern Analysis and Machine Intelligence* 31:306–318
37. Mei J, Liu M, Wang YF, Gao H (2016) Learning a mahalanobis distance-based dynamic time warping measure for multivariate time series classification. *IEEE Transactions on Cybernetics* 46:1363–1374

38. Quevedo J, Chen H, Cugueró MÀ, Tino P, Puig V, Garcíá D, Sarrate R, Yao X (2014) Combining learning in model space fault diagnosis with data validation/reconstruction: Application to the barcelona water network. *Engineering Applications of Artificial Intelligence* 30:18–29
39. Rakthanmanon T, Campana BJL, Mueen A, Batista GEAPA, Westover MB, Zhu Q, Zakaria J, Keogh EJ (2013) Addressing big data time series: Mining trillions of time series subsequences under dynamic time warping. *TKDD* 7:10:1–10:31
40. Roychoudhury S, Ghalwash MF, Obradovic Z (2017) Cost sensitive time-series classification. In: *ECML/PKDD*
41. Schäfer P (2014) The boss is concerned with time series classification in the presence of noise. *Data Mining and Knowledge Discovery* 29:1505–1530
42. Schäfer P, Leser U (2017) Fast and accurate time series classification with weasel. In: *CIKM*
43. Senin P, Malinchik S (2013) Sax-vsm: Interpretable time series classification using sax and vector space model. *2013 IEEE 13th International Conference on Data Mining* pp 1175–1180
44. Sharabiani A, Darabi H, Rezaei A, Harford S, Johnson H, Karim F (2017) Efficient classification of long time series by 3-d dynamic time warping. *IEEE Transactions on Systems, Man, and Cybernetics: Systems* 47:2688–2703
45. Smyth P (1996) Clustering sequences with hidden markov models. In: *NIPS*
46. Stefan A, Athitsos V, Das G (2013) The move-split-merge metric for time series. *IEEE Transactions on Knowledge and Data Engineering* 25:1425–1438
47. Yang D, Chen H, Song Y, Gong Z (2017) Granger causality for multivariate time series classification. In: *2017 IEEE International Conference on Big Knowledge (ICBK)*, pp 103–110
48. Ye L, Keogh EJ (2010) Time series shapelets: a novel technique that allows accurate, interpretable and fast classification. *Data Mining and Knowledge Discovery* 22:149–182